

## Effect of Alkane Adsorption on Electrochemical Properties of Graphene

Jie Tian, Yifeng Zhang, Xueqing Zuo, Chengwei Li, Zeng Fan\* and Lujun Pan\*

School of Physics, Dalian University of Technology, Dalian 116024, China

\*Corresponding author. E-mail: [fanzen@dlut.edu.cn](mailto:fanzen@dlut.edu.cn), [lpan@dlut.edu.cn](mailto:lpan@dlut.edu.cn)

### S1. AIMD Computational Details

All the AIMD calculations were performed with freely available CP2K/ Quickstep package.<sup>1</sup> The DFT implemented in CP2K is based on a hybrid Gaussian plane wave (GPW) scheme. The orbitals were described by an atom centered Gaussian-type basis set, and an auxiliary plane wave basis set was used to re-expand the electron density in the reciprocal space. The 2s, 2p electrons of O, 2s, 2p, 3s electrons of Na, 1s electron of H and 2s, 2p electrons of Na were treated as valence, and the remaining core electrons were represented by Goedecker–Teter–Hutter (GTH) pseudopotentials.<sup>2, 3</sup> The Gaussian basis sets were double- $\zeta$  with one set of polarization functions (DZVP),<sup>4</sup> and the energy cutoff was set to 400 Ry. We employed the Perdew–Burke–Ernzerhof (PBE) functional<sup>5</sup> to describe the exchange–correlation effects, and the dispersion correction was applied in all calculations with the DFT-D3 method.<sup>6</sup>

A matrix diagonalization procedure was used for the wave function optimization and the self-consistent field (SCF) convergence was facilitated by Fermi smearing with the electronic temperature of 300 K. In static calculations, the geometries were optimized by Broyden-Fletcher-Goldfarb-Shanno (BFGS) minimizer. For sampling the structures of the interface models and bulk solution, Born-Oppenheimer molecular dynamics (BOMD) was employed, and canonical ensemble (NVT) conditions were

imposed by a Nose-Hoover thermostat with a target temperature of 300 K. <sup>7</sup>The MD time step is set to 0.5 fs. Note that due to the large size of the supercells, only  $\Gamma$  point was used in all calculations.

## S2. MLP training

Based on AIMD, we trained a machine learning potential to describe graphene-alkane/water interfaces. We use the Deep Potential - Smooth Edition (DeepPot-SE), se\_e2\_a descriptor model to fit the potential energy surface (PES) for graphene - alkane/water interface, as implemented in the freely available DeepMD-kit package.<sup>8-</sup>

<sup>10</sup> The se\_e2\_a model uses two sets of deep neural networks (DNNs): the first DNN (the embedding net) maps the atomic configuration of atom  $i$  to a descriptor  $D_i$ , which encodes the 2-body radial and angular information within a cutoff radius ( $r_{\text{cut}}$ );  $D_i$  are then mapped to "atomic energy"  $E_i$  using a second DNN (the fitting net). The system total energy  $E$  is assumed to be the sum of atomic energies  $E = \sum_i E_i$ , while atomic forces  $F_i$  are derived from the negative gradient of the atomic energies  $E_i$ . MLMD using the se\_e2\_a model is interfaced with molecular dynamics engine LAMMPS,<sup>11</sup> as implemented in DeepMD-kit. See Sec. 2.2.5. for our LAMMPS MLMD details.

We construct 3 MLP models using a concurrent learning workflow implemented in the DP-GEN package,<sup>12</sup> with ab-initio trajectory as initial training set. We first randomly sample 1500 structures from the trajectory to train 3 initial models. Then, three consecutive steps, namely, exploration, labelling, and training, are repeated until MLP prediction reaches sufficient accuracy.

exploration: Several MLMD simulations at 300 K, 400 K, and 500 K are performed for configuration exploration. Here we use elevated temperature NVT simulation to enhance the PES sampling. Structures in these trajectories are classified as "accurate", "candidate" and "fail" according to model deviation, which is defined as the max force

deviation among 3 MLP models. (see ref<sup>13</sup> detailed descriptions for model deviation)

labelling: 50~100 "candidate" structures are selected for DFT labelling. These structures are added to the existing training set after DFT evaluations.

training: Use existing training set to train 3 MLP models again.

Below are the detailed DeePMD-kit and DP-GEN training parameters.

We use the `se_e2_a` descriptor model with local environment cutoff and smooth cutoff parameter set as 6.0 and 0.5 Å. The embedding net has hidden layers of size (20,40,80), and fitting net has hidden layers of size (100,100,100). The `axis_neuron` parameter for the descriptor is set to 16, which controls the embedding matrix size. (see ref<sup>10</sup>)

In each DP-GEN iteration, 3 MLPs are trained with 30000 steps, where the learning rate starts from  $1 \times 10^{-3}$  and finally decays to  $3.5 \times 10^{-8}$ . 300 K, 400 K and 500 K NVT ensemble sampling, are used for configuration exploration, where exploration time gradually increases from 2 ps to 10 ps. The upper and lower trust bounds for model deviation are set as 0.60 and 0.40 eV/Å, respectively.

For final production, 3 MLPs are trained with 120000 steps, where the learning rate starts from  $1 \times 10^{-3}$  and finally decayed to  $3.5 \times 10^{-8}$ .

### **S3. Molecular Dynamics Setting**

All MLMD simulations in this work are performed in the NVT ensemble with a time step of 0.5 fs using the LAMMPS package. We use the Nose-Hoover style thermostatting with temperature damping parameter of 100 fs. The initial configurations for MLMD are shown in Figure S4.

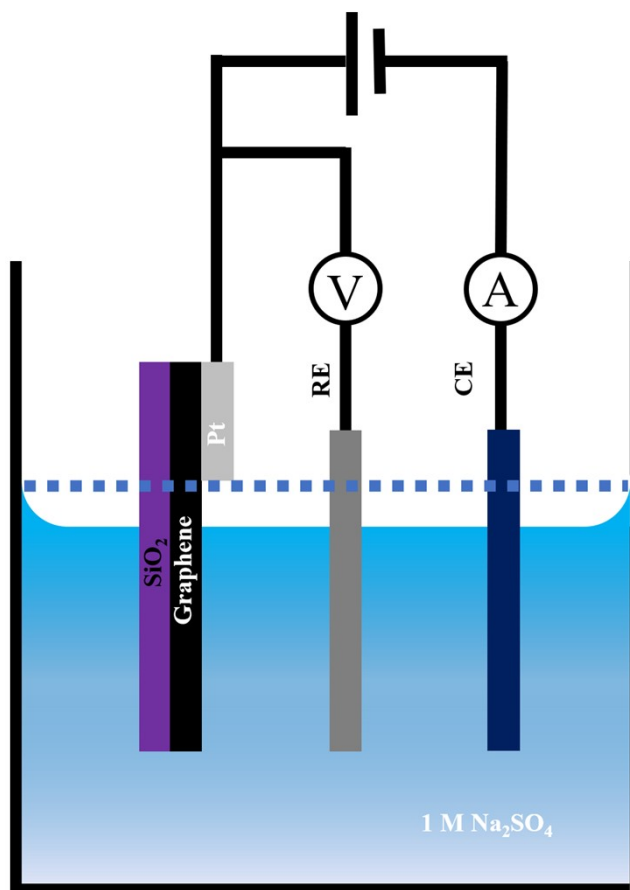
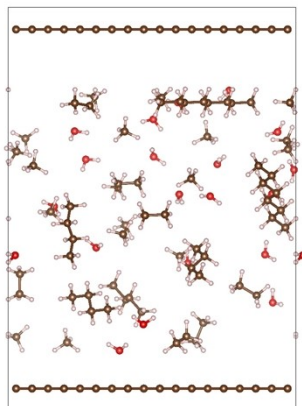
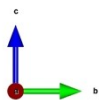


Figure. S1. Schematic diagram of electrochemical test device.

Initial state



Final state

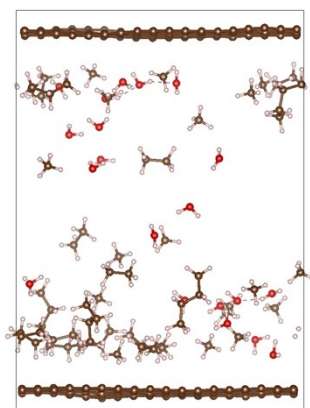
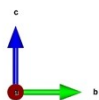
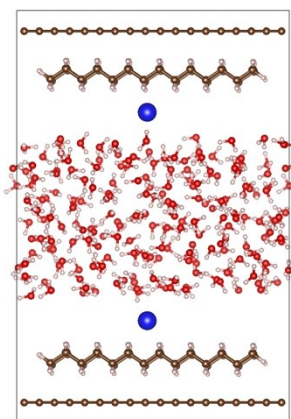


Figure. S2. Initial and final state of competitive adsorption models.

Initial state



Final state

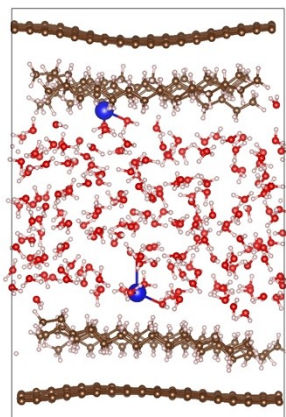
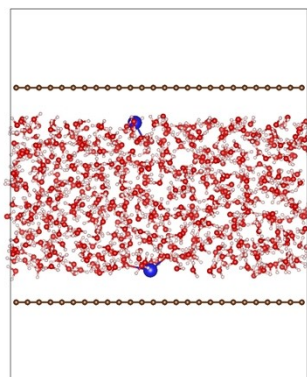


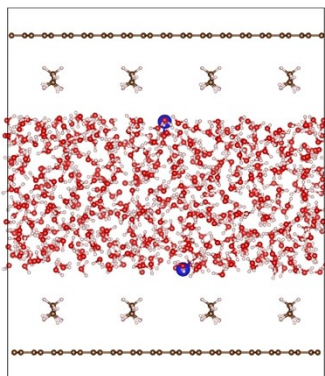
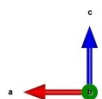
Figure. S3. Initial and final state of EDL models for AIMD.



Na1-C0



Na1-C0.5



Na1-C1

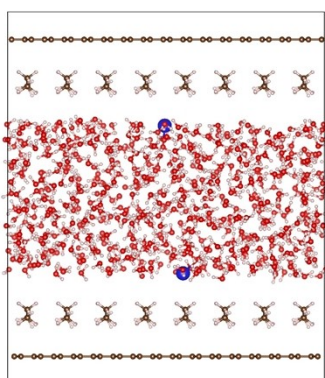
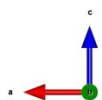
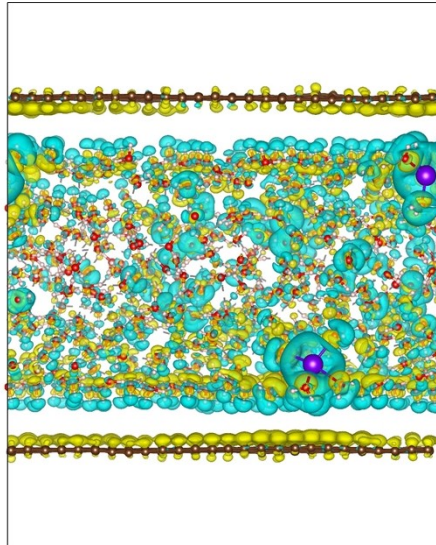
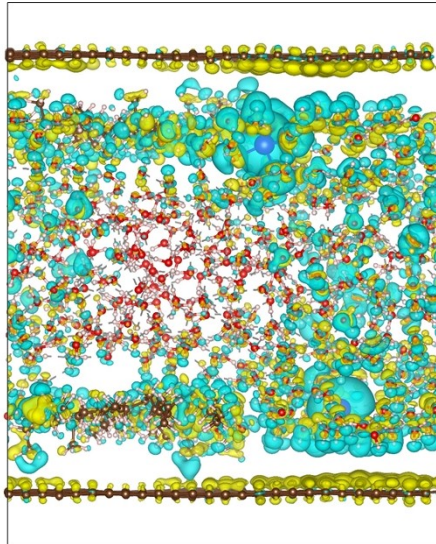


Figure. S4. Initial state of EDL models for MLMD.

Na1-C0



Na1-C0.5



Na1-C1

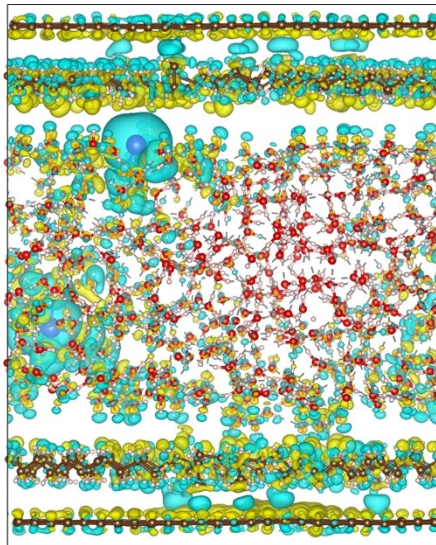
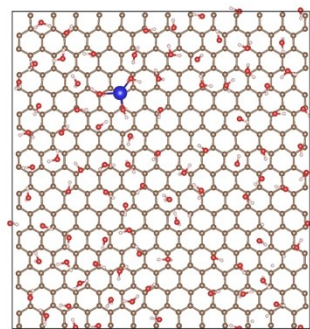
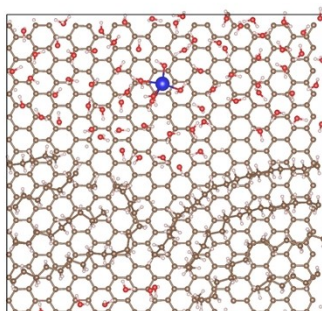


Figure. S5. Charge differential density profiles.

Na1-C0



Na1-C0.5



Na1-C1

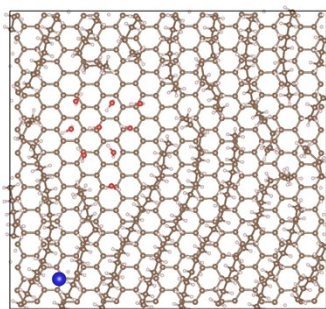


Figure. S6. The stabilized interface models

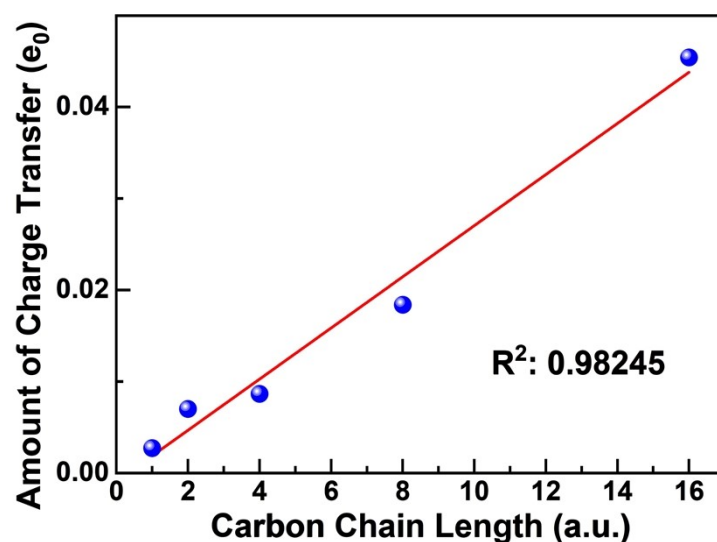


Figure. S7. The relationship between the amount of charge transfer and the length of the carbon chain.

## References

1. VandeVondele, J.; Krack, M.; Mohamed, F.; Parrinello, M.; Chassaing, T.; Hutter, J., Quickstep: Fast and accurate density functional calculations using a mixed Gaussian and plane waves approach. *Computer Physics Communications* **2005**, *167* (2), 103-128.
2. Goedecker, S.; Teter, M.; Hutter, J., Separable dual-space Gaussian pseudopotentials. *Physical Review B* **1996**, *54* (3), 1703-1710.
3. Hartwigsen, C.; Goedecker, S.; Hutter, J., Relativistic separable dual-space Gaussian pseudopotentials from H to Rn. *Physical Review B* **1998**, *58* (7), 3641-3662.
4. VandeVondele, J.; Hutter, J., Gaussian basis sets for accurate calculations on molecular systems in gas and condensed phases. *The Journal of Chemical Physics* **2007**, *127* (11).
5. Perdew, J. P.; Burke, K.; Ernzerhof, M., Generalized Gradient Approximation Made Simple. *Physical Review Letters* **1996**, *77* (18), 3865-3868.
6. Schröder, H.; Hühnert, J.; Schwabe, T., Evaluation of DFT-D3 dispersion corrections for various structural benchmark sets. *The Journal of Chemical Physics* **2017**, *146* (4).
7. Nosé, S., A unified formulation of the constant temperature molecular dynamics methods. *The Journal of Chemical Physics* **1984**, *81* (1), 511-519.
8. Zhang, L.; Han, J.; Wang, H.; Car, R.; E, W., Deep Potential Molecular Dynamics: A Scalable Model with the Accuracy of Quantum Mechanics. *Physical Review Letters* **2018**, *120* (14).
9. Wang, H.; Zhang, L.; Han, J.; E, W., DeePMD-kit: A deep learning package for many-body potential energy representation and molecular dynamics. *Computer Physics Communications* **2018**, *228*, 178-184.
10. Zhang, L.; Han, J.; Wang, H.; Saidi, W. A.; Car, R.; Weinan, E., End-to-end symmetry preserving inter-atomic potential energy model for finite and extended systems. In *Proceedings of the 32nd International Conference on Neural Information Processing Systems*, Curran Associates Inc.: Montréal, Canada, 2018; pp 4441-4451.
11. Thompson, A. P.; Aktulga, H. M.; Berger, R.; Bolintineanu, D. S.; Michael Brown, W.; Crozier, P. S.; in 't Veld, P. J.; Kohlmeyer, A.; Moore, S. G.; Nguyen, T. D.; Shan, R.;

Stevens, M. J.; Tranchida, J.; Trott, C. R.; Plimpton, S. J., LAMMPS - A flexible simulation tool for particle-based materials modeling at the atomic, meso, and continuum scales. *Computer Physics Communications* **2021**.

12. Zhang, L.; Lin, D.-Y.; Wang, H.; Car, R.; E, W., Active learning of uniformly accurate interatomic potentials for materials simulation. *Physical Review Materials* **2019**, 3 (2), 023804.

13. Zhang, Y.; Wang, H.; Chen, W.; Zeng, J.; Zhang, L.; Wang, H.; Weinan, E., DP-GEN: A concurrent learning platform for the generation of reliable deep learning based potential energy models. *Computer Physics Communications* **2020**, 253, 107206.